JOURNAL OF AIRCRAFT
Vol. 39, No. 3, May–June 2002

Aircraft Landing Impact Parametric Study with Emphasis on Nose Gear Landing Conditions

David H. Chester*
Israel Aircraft Industries, Ltd., 70100 Israel

A parametric approach to simulation of landing impact, with pitching and heaving degrees of freedom of the aircraft motion, has been used to determine the response of the main and nose gears. Compared to each gear's independent behavior, there are important differences in the landing conditions and in the resulting vertical loads and displacements when these aircraft motions are included. For main gears, the maximum vertical loads are almost linearly dependent on the sinking speed, but there is some variation in the proportion of kinetic energy absorbed. For nose gears, no similar validity exists, compared with the single gear results. Correlation with aircraft sinking speed is absent, but the response is sensitive to the values of initial pitch angle and pitch inertia. This is associated with the equivalent mass and its motion at this location, which are greatly affected by these input quantities and by the aircraft scale.

Nomenclature

$d(L/W)/dT_\eta$	=	rate of change of lift/weight ratio with pitch angle, 1/deg
E	=	energy absorbed by shock absorber and tire acting together, ft · lbf
F_h	=	hydraulic damping force coefficient of shock absorber, lbf/(ft/s)^2
g	=	acceleration of gravity on the Earth's surface, nominally 32.2 ft/s^2
I	=	polar moment of inertia of aircraft, taken about the center of gravity, slugs · ft^2
K	=	slope of line through endpoints of force/displacement curve (Fig. 2), lbf/ft
k	=	radius of gyration in pitch, $\sqrt{(I/W)}$ ft
L/W	=	ratio of the aircraft lift force to its weight
L_1	=	horizontal distance along aircraft between nose and main gears, ft
L_2	=	horizontal distance along aircraft between the center of gravity and the main gear, ft
L_3	=	height of the center of gravity from the ground line, when gears are fully extended, ft
n_z	=	normal load factor at center of gravity
T_η	=	angle of tail-down pitch, from the horizon, deg
$T_{\eta 0}$	=	initial value of T_η at moment of touchdown, deg
t	=	elapsed time from touchdown, s
V	=	vertical force on one landing gear, lbf
V_{fs}	=	forward speed of aircraft, ft/s
V_{ss}	=	sinking speed of aircraft at moment of touchdown, ft/s
W	=	mass of aircraft, slug
z	=	vertical displacement (compression) of landing gear (tire and shock absorber), ft
Δn_z	=	increment of vertical load factor (without lift), due to landing gear dynamic loads, g
ϕ	=	downward slope of flight path, $\arcsin(V_{ss}/V_{fs})$, deg

Subscripts and Superscript

e	=	equivalent mass at nose
m	=	main landing gear
n	=	nose landing gear
sn	=	static condition
1, 2 (with z)	=	first or second derivative of displacement with respect to time
,	=	normalized to the scale of the baseline aircraft

Introduction

IN a general sense, the analytical solution of aircraft landing impacts has received very little attention, within the broad range of its dynamic behavior. One reason for this neglect is that during the more common tail-down landings, all of the weight is first carried on the main gears. When the most critical landing conditions and loads on these gears are determined, a simplification is often made. It is reasonably but inaccurately assumed that there is no need to include the pitching motion of the aircraft and the response of the nose gear. This attitude also prevails within Part 25 of the airworthiness standards[1] (also known as FAR Part 25), which call for main gear simulation and dynamic testing without considering the response of the rest of the aircraft. Only its mass and the external landing conditions are required as input. The use of aircraft elasticity effects (which are mostly beneficial to reducing the loading) has only recently been allowed into the simulations for determining the main gear design loads, according to the latest version of the requirements in FAR Part 25.[1] Pitching (free-body) motion also confers the same kind of benefit, but it is not prescribed, nor are its effects usually included.

When the nose gear landing impacts, the situation is not taken very seriously either. On most aircraft, only about 10% of the total weight is carried there. These gears are still regarded as supplementary and auxiliary in the regulations, an inheritance from the days of the tail skid (see paragraphs 23.497–23.499 and 23.509 in Part 23 of Ref. 2). The landing conditions that are taken as applicable to nose gears are modifications of those used on main gears, with the same sinking speeds and an effective mass that is a function of longitudinal deceleration and center of gravity height (see Refs. 1 and 2 paragraphs 725). These assumptions and methods of finding the landing-impact conditions at the nose are inappropriate. In particular, the formula used for determining the effective mass is unrealistic, and (as shown by Buxbaum,[3] for example) the effect of this mass on the loads was not properly understood.

Presented as Paper 4-11-2 at the ICAS Structural Dynamics Session Conference at Harrogate, UK, August 2000; received 22 April 2001; revision received 30 September 2001; accepted for publication 10 December 2001.

*Senior Engineer, Structural Analysis Department 4441, Engineering Division, Ben-Gurion International Airport.

When this is applied to the fatigue loads spectrum, it is necessary to take the average conditions and to use factual values of loads, based on experience. Consequently, the design criteria that are specified in FAR Part 25 (Ref. 1) (after a suitable adjustment to more typical sinking speeds) can scarcely be considered as a suitable means for determining the actual landing conditions, nor are they satisfactory for finding the resulting loads felt by an aircraft that is being tested or is in use. A complete simulation of the aircraft motion is the means needed to overcome these inaccuracies.

However, not all aircraft and their gears behave in the same way, and the large range of possibilities in size, weight, and motion complicates the situation. To understand the implications of what different aircraft provide in the way of landing gears and what these gears do to the aircraft, their landing characteristics must be examined parametrically.

Description of Parameters

The British (Imperial) system of physical units will be used throughout this work. Lengths are taken in feet, masses are provided in slugs and time passes in seconds. The mass unit of one slug is preferred, because it causes a force of one pound to be felt when the associated acceleration is 1 ft/s^2, with the result that one slug weighs 32.2 lbf., when this state of equilibrium is reached on the Earth's surface.

Choice of the Base-Line Aircraft and its Landing Condition

In this parametric study, it is first assumed that all of the aircraft under consideration have their landing gears arranged in a nose wheel (or tricycle) layout with their main gears located behind the center of gravity (Fig. 1). Because this is the most common configuration, it is the behavior of the aircraft having this kind of gear array that is of interest. Even though not all aircraft necessarily adhere to the formal tricycle layout, the results of this motion study may still be applicable.

The performance of the aircraft in pitch and heave, together with the influence of its sinking (and forward) speeds, is to be examined. Consequently, the kinds of data used here are related to these directions only. The following aircraft properties are taken as input data to the simulation program. Their number has been restricted, with the aim of simplification, by only using those that are absolutely necessary.

Mass Properties

The size of the starting configuration is chosen as a geometric mean between the smallest and largest sizes of aircraft being covered by the study. The range in capacity lies between landing weights of aircraft of almost the ultralight magnitude of 1610 lbf (50 slugs) and of the jumbo-jet capability of 644,000 lbf (20,000 slugs). Hence, the baseline mass is $W = 1000$ slugs (which corresponds to an aircraft weight of 32,200 lbf). Thus, the smallest aircraft being considered is $\frac{1}{20}$ of the baseline mass and the greatest is 20 times this value.

The other mass-dependent property of importance is the moment of inertia in pitch about the center of gravity. This quantity depends on the proportion of fuel mass being carried, mostly at or near the center of gravity, compared to the payload mass, which is usually centered slightly ahead of this position and spread along the length of the fuselage. A pitching moment of inertia $I = 144{,}000$ slug ft^2 is a typical for a passenger-carrying aircraft of the baseline size. In this case, it is due to a radius of gyration of the mass of $k = 12$ ft, which is slightly less than half the longitudinal separation of the gears L_1 (see following section).

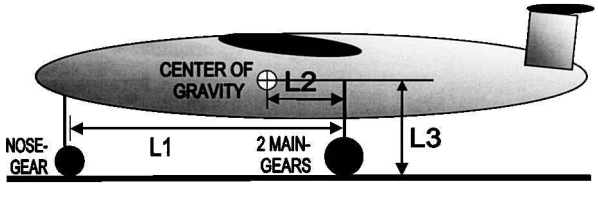

Fig. 1 Choice of baseline aircraft parameters; mass: W = 1,000 slug (32,200 lbf weight), 20 times light aircraft size (1,610 lbf), and $\frac{1}{20}$ of size of a jumbo jet (644,000 lbf) and geometry: horizontal spacing between gears, L_1 = 30 ft, proportion of static weight carried on nose gear, L_2/L_1 = 0.10, and height of center of gravity from ground line without load on gears, L_3 = 7.5 ft.

Geometric Properties

It is assumed for such an aircraft that the fore/aft distance between the main and nose gears is $L_1 = 30$ ft, with the center of gravity located at 10% of this spacing, or $L_2 = 3$ ft ahead of the main gear. For ease of analysis, the legs of the gears are arranged to be at right angles to the horizontal reference line of the aircraft, which itself is parallel to the ground, when the gears are fully extended. This aircraft is assumed to have its center of gravity at a height $L_3 = 7.5$ ft from the ground line in this condition. The significant geometric properties are shown in Fig. 1. No sideways dimensions are included because we are concerned only with variations in the longitudinal/vertical plane of symmetry.

Vertical Load/Deflection and Damping Characteristics

The deflections of the shock absorbers and tires are taken as acting together as a combined system. For the baseline aircraft, the total compressions of these two components on both main and nose landing gears is $z = 1.2$ ft at the ultimate condition of full closure. Because the greatest vertical forces here are due to the reserve-energy test case of impact (see FAR Part 25 (Ref. 1), paragraph 25.727), the associated decelerations (for an assumed 75% efficient compression of the combined systems) can be shown to be $\Delta n_z = 2.485\ g$. Thus, the ultimate vertical force on each of the two main gears, assuming that on impact they take all of the vertical kinetic energy, is V_m maximum = 40,009 lbf (Fig. 2). Consequently, the linearized endpoints stiffness of the main gear is $K_m = 40{,}009/1.2 = 33{,}341$ lbf/ft.

For the nose gear, it might be supposed that the loading conditions are directly proportional to those at the main gear when the "static" mass is taken. However, in practice, nose gears are made considerably stiffer than this. The reason for this will be appreciated later when the associated landing conditions are better understood. Meanwhile, it is tentatively assumed that the maximum vertical force that this gear is designed to carry is 40% of that taken by one of the two main gears and not 1/4.5 or 22.2% of the main gear's value, which otherwise would be the case without this changed assumption. Then, for the same motion and deceleration, the ultimate vertical force at the nose gear is $V_{n\,\max} = 16{,}004$ lbf (Fig. 2), and the associated endpoints' stiffness is $K_n = 13{,}337$ lbf/ft.

These stiffnesses are not in proportion to the static loads on the respective gears, and consequently, when standing with its weight on the ground, the nose gear shock absorber is the more extended one. When the length of the rest of this gear is shortened, it can easily be arranged for the aircraft to be at a level attitude on the ground for a particular weight and center of gravity position. The actual load/displacement curves, for the shock absorbers and tires on the main and nose gears, will be assumed to have the same geometric form, which is in accordance with the gas compression laws of these two kinds of compressing elements. This in keeping with

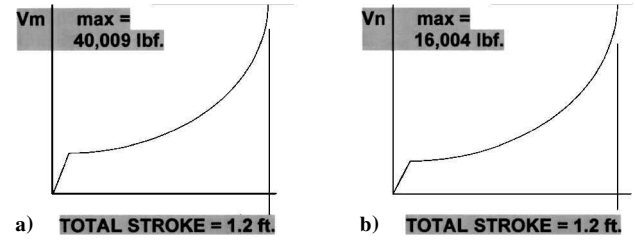

Fig. 2 Compression curves of shock absorbers and tires; maximum compression load for reserve energy drop test at 12 ft/s sinking speed, when compressive efficiency is 75% (Δ_{n_z} = 2.485 g): a) main shock absorbers, overall stiffnesses K_m = 33,341 lbf/ft and hydraulic damping coefficients F_{hm} = 400 lbf/(ft/s)^2 and b) nose shock absorber, K_n = 13,337 lbf/ft and F_{hn} = 160 lbf/(ft/s)^2.

current design practice, where only minor differences are introduced between the shapes of these compression curves.

During landing impact, the shock absorbers (a typical arrangement is shown in Fig. 3) will also develop internal hydraulic damping forces. These forces are assumed to be produced by fixed-size orifices, where the pressure change across each is proportional to the square of the velocity of compression. No allowance for variable-sized metering pins is made; for our purposes, this is a less significant effect. The hydraulic damping coefficients are chosen at the design (limit-load) conditions of Ref. 1 paragraph 25.473, where the maximum closure rate of 10 ft/s causes the same amount of hydraulic force (oil peak) as results from the subsequent maximum gas compression. This is developed close to the end of the stroke (see earlier discussion), when the closure velocity is zero. Consequently, the hydraulic damping coefficient of the main gears works out to be $F_{hm} = 400$ lbf $\cdot$ (ft/s)^2, and for the nose gear, this coefficient is $F_{hn} = 160$ lbf $\cdot$ (ft/s)^2. From simulations performed at the reserve-energy ultimate design condition of 12 ft/s sinking speed [on drop testing (see Ref. 1, paragraph 25.723)], the greater hydraulic and gas compression forces also are roughly equal in size.

During the return stroke, the positive recoil orifices that are fitted to the shock absorbers are assumed to develop forces that are four times these values. This is regarded as a reasonable approximation to the design situations that occur in practice.

Aerodynamics

The design value of the tail-down angle of pitch T_η is usually made to correspond to the condition where the rear fuselage just scrapes the ground at the fully extended position of the main gears. For aircraft with relatively short fuselages, this angle is made to correspond with the stalling angle, as called for in paragraph 25.481 of the FAR Part 25 (Ref. 1) requirements. However, in practice, when an aircraft lands, the tail-down pitch angle is not as high as the design value, and actually most aircraft are pitched to an angle T_η of about 5 deg at the instant of touchdown (in Ref. 4, for example). The baseline aircraft initial value of $T_{\eta 0} = 5.5$ deg is assumed here as being typical.

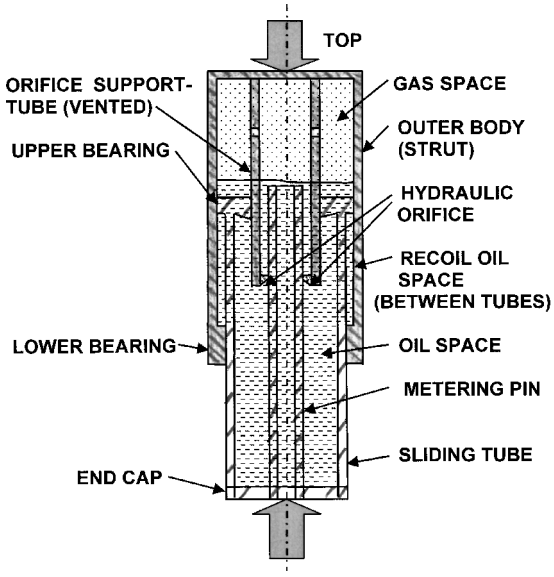

Fig. 3 Longitudinal cross section of a typical oleo-pneumatic shock absorber.

The aerodynamic properties of the aircraft in lift result in this force almost being equal to the weight. This quantity is not made exactly equal to it because, during the landing sequence, the pilot wants to avoid floating just above the runway, for an extended distance. Consequently, in practice the pilot deliberately chooses a lift/weight ratio L/W that is slightly less than one, and the value of 0.90 is assumed here. As the landing proceeds, the pitch angle changes and, associated with this, so does the lift on the wing. It is assumed that the variation with pitch angle is linear and that the value of the derivative $\mathrm{d}(L/W)/\mathrm{d}T_\eta = 0.10$/deg. There are no other kinds of aerodynamic forces used in this analysis. The balance in pitching is caused by the turning moments from the tail plane and elevator forces being in opposition to the moments from the lift at the aerodynamic center. It is assumed that this balance is maintained as the motion proceeds. This simplification is not far from what actually occurs during a landing, when the dominant effect of the vertical reaction on the main gears (together with the reduced forward speed) result in the nose of the aircraft tending to pitch down (Fig. 4, stage b).

The associated horizontal ground speed on touchdown depends on the head wind, as well as the size of the lifting surfaces and flaps. For the baseline aircraft, a ground speed of 104 kn or $V_{fs} = 176$ ft/s is assumed as a likely value. The average sinking speed during landing is less than $V_{ss} = 3$ ft/s for many aircraft.[4] This should be compared with the usual design value for a once in a lifetime occurrence operation of $V_{ss} = 10$ ft/s according to the design requirements in FAR Part 25.[1] A range of values of this quantity will be used in the simulations to be presented.

Kinematics of Flight

The pilot performs a flare maneuver or roundout from the final approach flight path (which by international agreement is nominally at 3 deg of slope). The pilot then lands with a small but positive sinking speed after the start of the runway. However, this finite sinking speed causes the total aerodynamic angle of attack to exceed, by a small amount, the nominal value of $T_{\eta 0} = 5.5$ deg of pitch-up angle of the nose. For an assumed average sinking speed $V_{ss} = 2.5$ ft/s, this influence on the angle of attack is equal to $\phi = \arcsin(2.5/176) = 0.82$ deg. Hence, the actual angle of attack in our case would be 6.32 deg. Even when the sinking speed is much greater, the angle of attack will not differ much from this value. This is because the lift/weight ratio is held close to unity, and the lift depends primarily on the forward speed. The pilot maintains this speed slightly in excess of that of the stall. Consequently, it is the pitch angle that is varied at high sink rates. In the case of the sinking speed $V_{ss} = 10$ ft/s, the increment in angle from this flight-path kinematic feature is $\phi = \arcsin(10/176) - 0.82 = 2.44$ deg and, hence, the value of $T_\eta = 5.5 - 2.44 = 3.06$ deg. This reduction of pitch angle during landing at high rates of sink helps to explain how nose

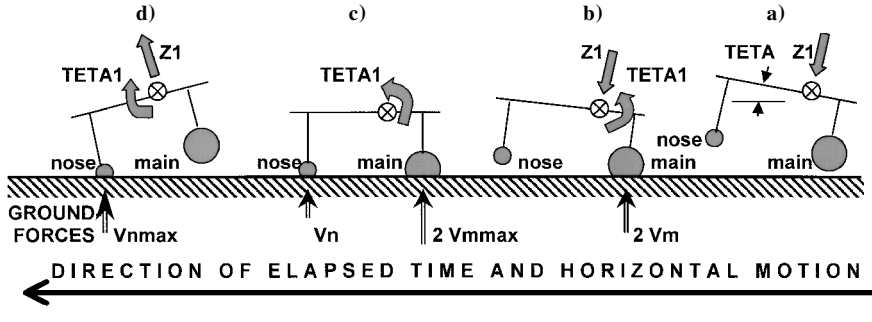

Fig. 4 Landing process (heavy tail-down impact): stage a, initial condition on touchdown, all gears in air; stage b, main gears impact and nose pitches down; stage c, impact of nose gear, main gears start to recoil at maximum loads; and stage d, nose gear at maximum load, main gears bounce into the air.

gear landing impacts sometimes precede the main gear impacts, with disastrous results in certain cases (see Ref. 5).

Simulation Procedure

Description of Computer Program

The basic principle used in this procedure is the integration of the equations of motion in heave and pitch. The simulation of the motion commences at the point of tire touchdown. The initial conditions of the variables are set to represent this stable point on the flight path. The integration then proceeds, performed according to the predetermined motion of the aircraft and its variable geometric and mechanical constraints. These forces depend on the displacements of the main and nose landing gears and also on the lift characteristic. The forces and turning moments that result are used together with the mass properties to obtain the current vertical and angular accelerations. On integration, these provide the succeeding velocities and displacements for the next cycle of calculation.

The various stages of the program are shown in the flow chart of Fig. 5. The program starts by reading the input data, most of which has been described earlier. After the sizes of the tables have been specified, the shock absorber and tire compression characteristics are input in their tabular forms. In addition, some zero values of the initial conditions of motion are read. The anticipated duration of the simulation is also input, together with the increment of time to be used for each calculation step. The program echo prints all of these data. It subsequently prints the titles for the output results. Before the iteration loop is started, certain quantities are fixed for subsequent use.

After entering the loop, the first set of printed output results at time $t = 0$ does little more than confirm that the initial conditions have been correctly set. For the cycle that follows, the initial compressions are found from the sinking speed multiplied by the time increment. These displacements are introduced into a subroutine for interpolating from the look-up tables, to obtain the values of the gear compression forces. These forces and their associated pitching moments then are applied using Newton's second law of motion to determine the accelerations in heave and pitch. Integration of these values provides the velocities and displacements that are needed for use during the subsequent iteration. As the calculation proceeds, changes are made to the geometry of the positions of the landing gear forces. This and other motion-dependent effects are included in the later cycles. Each cycle, after the first, starts by printing out a set of results gathered from the previous set of calculations.

In the usual case of a tail-down landing, the results of this analysis show the manner of development of the vertical forces at the main gears together with their displacements and motions. Subsequently, the nose-down pitching causes the nose gear to strike the ground and the vertical and pitching motions to eventually reverse their

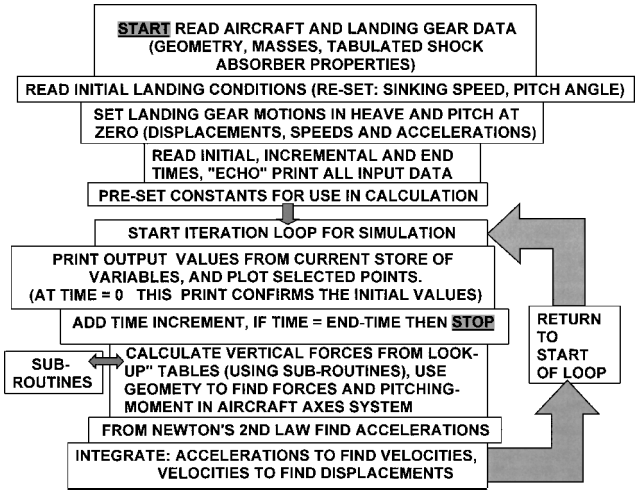

Fig. 5 Flow chart of the computer program for simulation.

directions. Should the full stroke of the shock absorbers and tires be exceeded, the gear "bottoms" and the simulation stops prematurely, after supplying an appropriate comment.

By the use of a number of simulations having progressively smaller time intervals, it is possible to determine the interval below which no significant improvement in the accuracy of the results may be obtained. This procedure was used for all of the work to follow, with the errors held to no more than 2.5%. This accuracy is regarded as sufficient because the aim of this study is to show the chief trends of the various output forces and motions, with the variation of particular input parameters.

Results of the Simulation: Description of the Landing Process

The results of a typical simulation contain the following stages in the symmetric landing motion, which are also illustrated by the four diagrams in Fig. 4.

At the initial landing condition, lift almost equals weight, but there is a finite sink rate. The aircraft is balanced in pitching without angular motion. The pitch angle is small and positive, causing a component of sinking speed along the gears' compression axes to exceed slightly that of the aircraft. The wing angle of attack is greater than the pitch angle by a small amount that is proportional to the ratio of sinking and forward speeds.

On impact, the main gears start to compress. The vertical loads on them grow and cause the aircraft to pitch nose down, that is, at a negative rate. The decreasing angle of pitch has the effect of reducing the aerodynamic generated lift/weight ratio. Kinetic energy from the mass and sinking speed is absorbed within the main shock absorbers together with some potential energy, due to the subsequent loss of balance between lift and weight.

The vertical loads on the main gears first reach peak values, due to the maximum velocity of the shock absorber closures, causing their internal hydraulic damping forces to dominate. With the subsequent reduction of this speed but continued closure, it is the turn of the gas compression characteristics to cause a second peak to occur in the time history of the shock absorbers' vertical forces. At this moment, the vertical motion is arrested. The peak in loading is simultaneously felt at the axles and on the ground.

The motions of the main shock absorbers then reverse. Because of the internal friction, a step reduction occurs in the time history of the axial forces. These continue to reduce with time as this motion proceeds. The aircraft does not normally bounce back into the air, sufficiently large recoil damping having been provided by the secondary hydraulic orifices.

After a delay that depends on the initial conditions, the negative rate of pitching motion causes the nose gear to strike the ground. (It is assumed that there is no change in the aerodynamic pitching moments due to the pilot's control or other ground-related influences.) The pitch angle of the aircraft at this instant is close to zero. It may even be negative because the main gears can have already started to extend. The nose gear impact combines the momentum of the vertical motion (not fully absorbed at the main gears) with rotation. This angular motion is due to the inertial response of the aircraft to the pitching moment supplied from the main gears' reactions. After the nose gear has landed, this energy in aircraft pitching motion is transferred into the nose gear shock absorber, and the aircraft's negative pitching motion is arrested and eventually reversed.

The nose gear experiences the same kinds of internal load time history as the main gears, with the hydraulic and gas load peaks being developed in turn. Depending on the conditions on nose gear landing, a clear separation between these peaks does not necessarily occur in practice.

When the momentum is transferred to the nose, there are reduced reactions on the main gears. However, after the pitching rate is reversed, these loads increase again. Although it is not provided in this numerical analysis, a second cycle of heaving and pitching motion results, with associated increases in the wing lift, too. Compared to the first cycle, the size of these motions and the changes in the forces are diminished.

The braking forces and aerodynamic drag help to reduce the horizontal speed of the aircraft. Eventually, the reactions on all of the

gears reach their static values without lift, after all of the energy of the motion has dissipated.

Numerical Simulations

Choice of Input Parameters

The effects of variation of the various physical quantities are explored here. Our process of investigation is now applied to the following kinds of input parameters: 1) initial pitch angle (tail-down angle) $T_{\eta 0}$, 2) aircraft sinking speed on touch down V_{ss}, 3) aircraft radius of gyration in pitch about the center of gravity $k = \sqrt{(I/W)}$, and 4) relative scale or size of aircraft (compared to baseline aircraft) W.

The first three kinds of these parameters are relatively straightforward, and their variation is considered to apply independently. However, in the case of the last parameter, aircraft relative scale, a number of these different input quantities change in combination with the mass W, which is regarded here as the basic measure of the scale of the aircraft.

The geometry of the aircraft and of its landing gears are both related to the relative scale. This term is expressed through the mass compared to that of the baseline aircraft. The geometric changes are determined as follows.

1) The first set of parameters are horizontal lengths along the fuselage, which affect the spacing between nose and main landing gears L_1, the position of the center of gravity L_2 from the main gear, and the pitching inertia expressed by the radius of gyration k. These three quantities are assumed to vary according to the cube root of the aircraft mass W (assumption of constant density).

2) Vertical height of the center of gravity L_3 varies according to the sixth root of the mass, and not by the preceding rule. This variation in the height of the center of gravity is less than in the case of the horizontal distances. This result is found to be closer to the way that actual aircraft are designed.

3) The same variation with mass applies to the horizontal landing speed V_{ss}. According to the classic theory, the quantity should obey the famous squared–cubed rule, but in practice the wing loading of the smaller aircraft is lower, the degree of refinement for high lift coefficients also becomes less, and this is the overall result.

4) The strokes of the shock absorbers and the compressions of the tires z vary according to the relative size (mass) raised to the power of one-fifth.

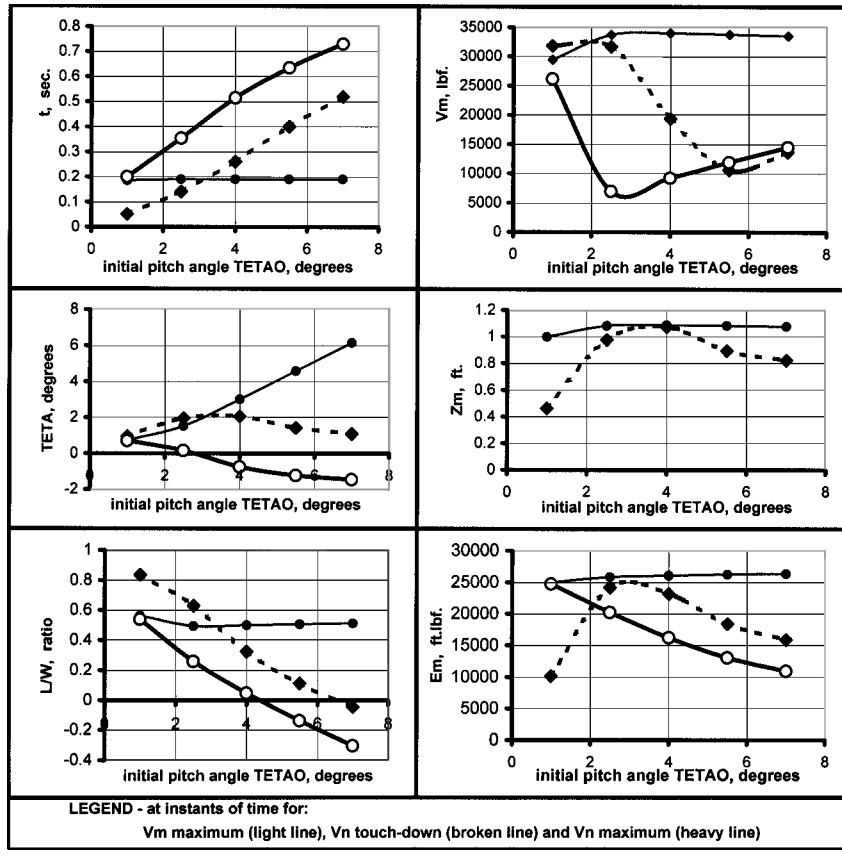

Fig. 6a Effect of initial pitch angle on motion, forces, and energy absorption on main landing gears.

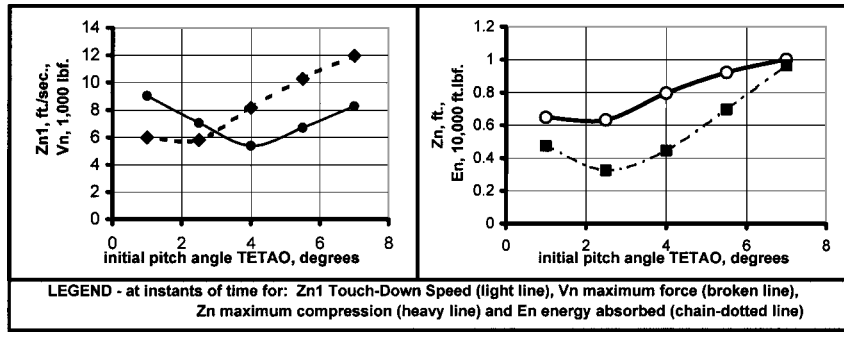

Fig. 6b Effect of initial pitch angle on motion, forces, and energy absorption on nose landing gear.

This latter quantity is related to the energy absorbed by the landing gears during the landing impact, which itself depends directly on the mass, without any allowance for changes to the design sinking speed. Consequently, the magnitude of the forces in the shock absorbers will vary according to the mass when raised to the power of four-fifths. This ensures that the various shock absorbers being considered are comparable as energy absorbing elements. This stroke criterion of mass raised to the power of one-fifth has been deliberately introduced here, so that for the 20 times greater scale aircraft, the length of the stroke corresponds to that found on the jumbo jets of about 2.2 ft. Then for the baseline aircraft scale, the stroke is 1.2 ft, and for the ultralight lowest aircraft scale that is $\frac{1}{20}$ of the basic size, the stroke of about 0.66 ft is used. All three values of these strokes are quite typical of design practice, and the associated maximum compression loads also correspond.

Description of Results from the Simulations

A number of aircraft landing simulations were run on the computer, and the resulting outputs were obtained in the form of time histories. This output included the gear displacements, velocities, and accelerations, together with the associated forces and absorbed energies. In terms of the design conditions and their criteria, the author's previous experience in working with these outputs has shown that there are three points in the time history that are of importance. These are at the maximum gas compression force in the main gear, at the instant of nose gear touchdown, and at its maximum gas compression force.

To appreciate these output data in parametric terms, the summarized results are presented graphically in Figs. 6–9, and a description of their main features is given below.

Effect of Variation of Initial Pitch-Angle (Tail-Down Angle) $T_{\eta 0}$

This variation is shown in Fig. 6. This variable has a large influence on the results. The first graph shows that the time taken for the nose gear to reach the ground is linearly proportional to the initial value of $T_{\eta 0}$. Although the maximum vertical forces on the main gear are scarcely affected, there is a large variation in the subsequent pitching motion and in the force when the nose gear first touches down and later when it reaches its maximum value. At the time of main gear maximum vertical load, the variation of lift/weight ratio L/W with initial angle of pitch is virtually nil. Later when the nose gear is involved, this ratio varies linearly in the opposite

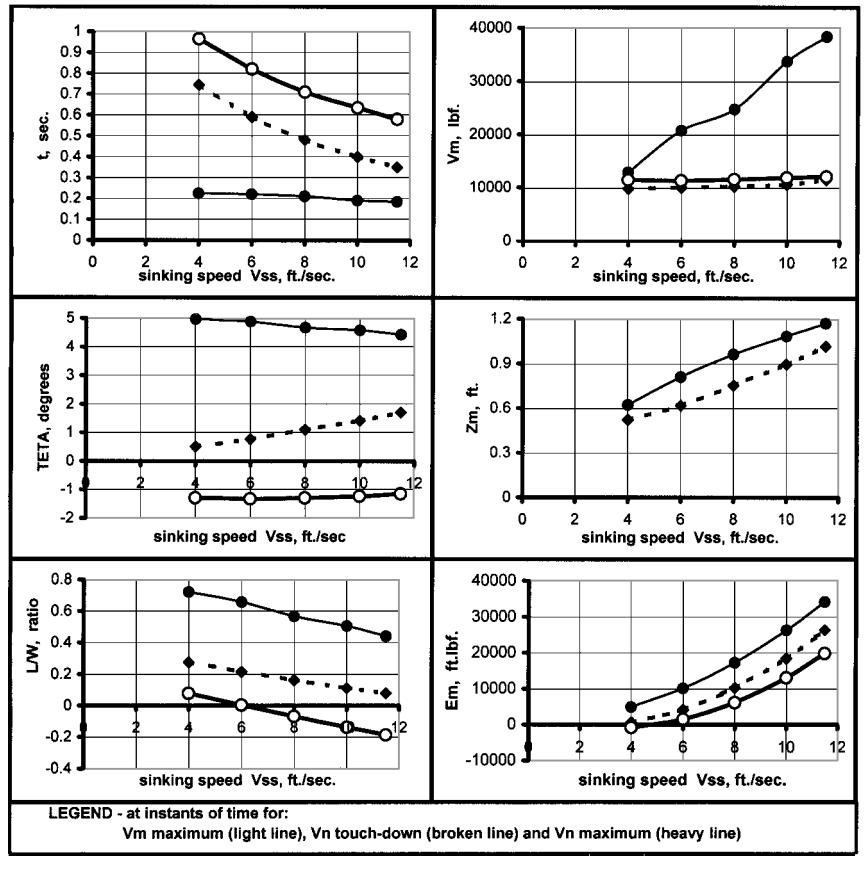

Fig. 7a Effect of sinking speed on motion, forces, and energy absorption on main landing gears.

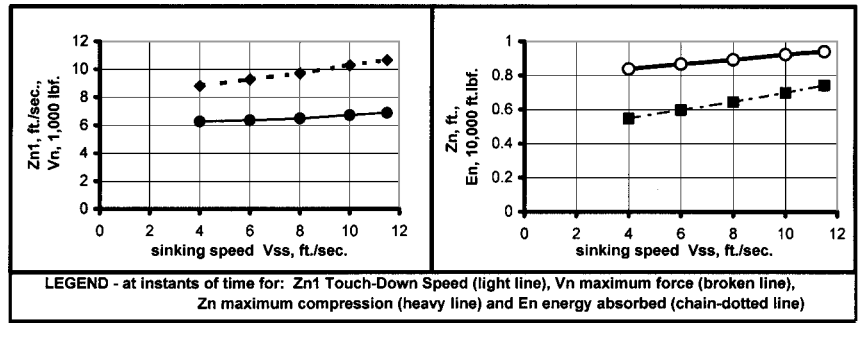

Fig. 7b Effect of sinking speed on motion, forces, and energy absorption on nose landing gear.

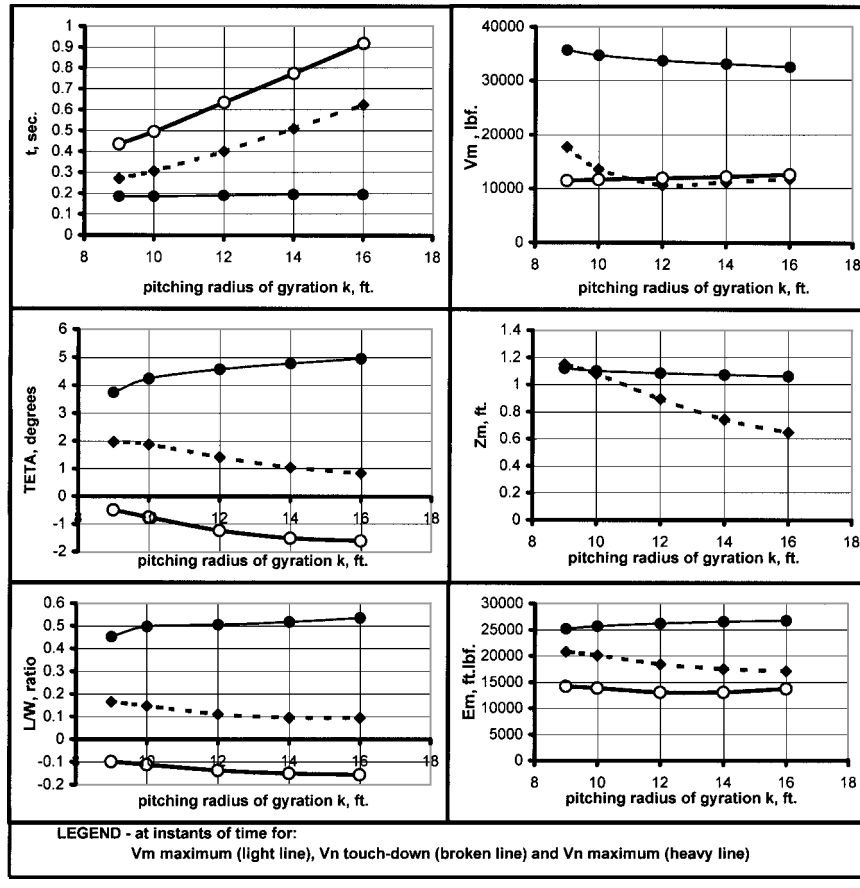

Fig. 8a Effect of pitching moment of inertia on motion, forces, and energy absorption on main landing gears.

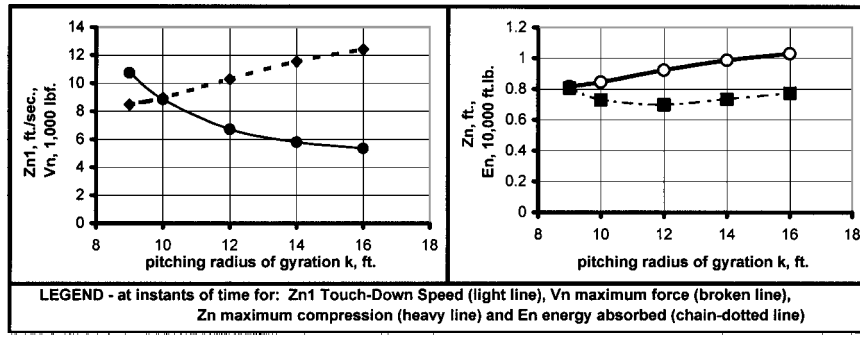

Fig. 8b Effect of pitching moment of inertia on motion, forces, and energy absorption on nose landing gear.

direction, with the greatest values present when the initial angle is small. At the time when the nose gear reaches its maximum load, the main gear takes progressively larger amounts of the total energy for smaller values of $T_{\eta 0}$. However, there is a maximum amount absorbed in these gears at the instant of nose gear first touchdown for an intermediate value of this angle. The energy in one leg sometimes exceeds half of the total kinetic energy at the initial impact of $E_{m0}/2 = 25{,}000\,\text{ft} \cdot \text{lbf}$ on the baseline aircraft, due to conversion of some of the potential energy taken from the height of the center of gravity at initial touchdown.

The slam-down vertical force on the nose gear from large pitch angles is smaller than the maximum loads it experiences from level landings. However, the velocity of this landing (which is about 90% of the main gear design value) is the same at the extreme angles of pitch, with a minimum intermediate value that is considerably less. As already noted, for the main gear this corresponds to a maximum energy absorption peak. On the specific nose gear used here, the energy absorbed from the slam-down maneuver and the associated maximum vertical forces are greater than for level landing, and the general situations due to this operation should not be so easily dismissed as has been formerly done.

Effect of Variation of Sinking Speed V_{ss}

This is shown in Fig. 7. Unlike the earlier kind of variations, there is a continuous change in the output results without any intermediate maximum values being developed, a result that is expected. Of particular interest is the almost linear variation of the maximum vertical load on the main gears with sinking speed. Because the damping forces and the compression curve are both nonlinear, the manner by which they absorb the energy results in the described linear effect. The other surprise here is that on the nose gear there is almost no variation with the initial sinking speed of the aircraft and only a small change in its associated absorbed energy. For the particular set of input data used, the initial velocity of nose gear touchdown is almost constant at about 6.8 ft/s. The only explanation for this lack of sensitivity is due to the moderating effect of the initial pitch angle,

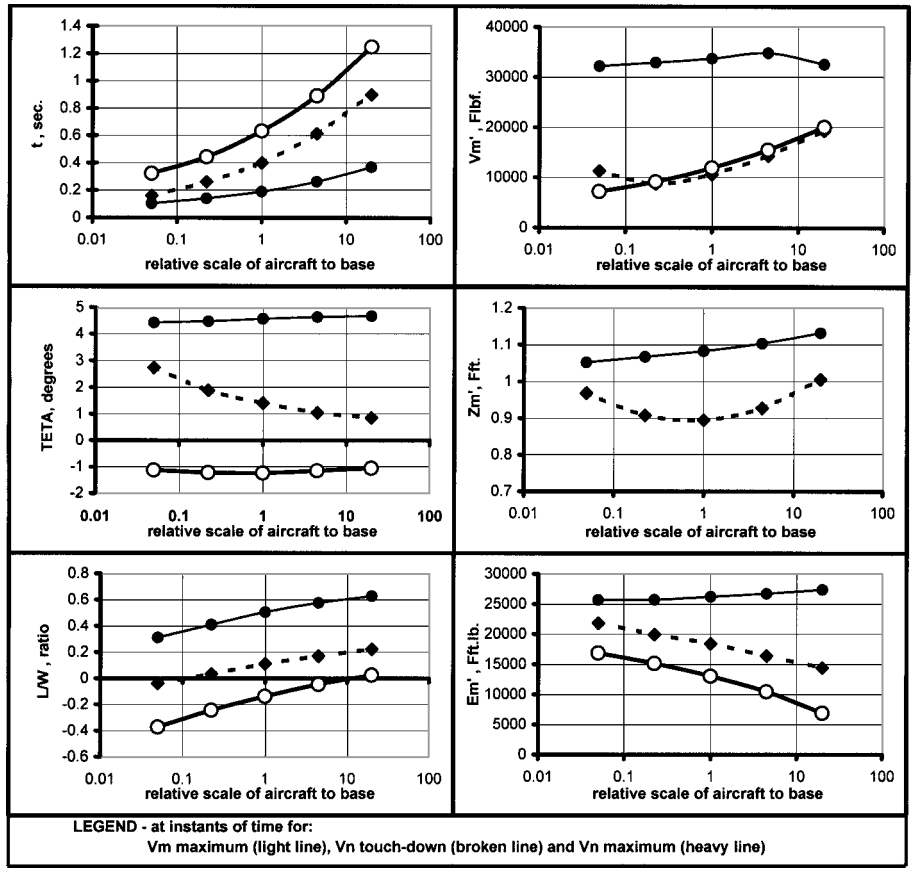

Fig. 9a Effect of aircraft scale on motion, forces, and energy absorption on main landing gears.

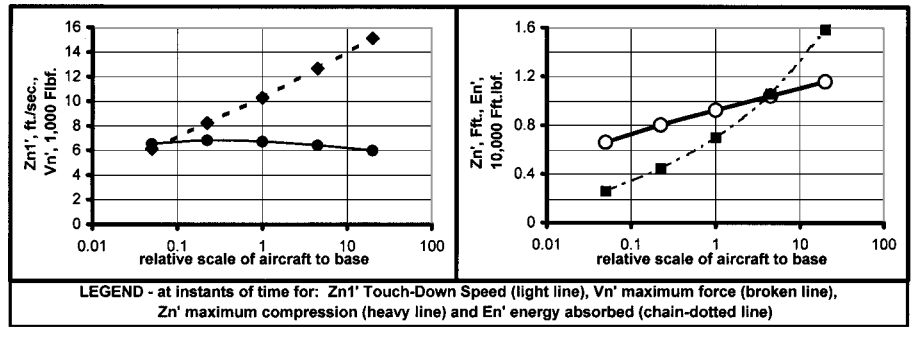

Fig. 9b Effect of aircraft scale on motion, forces, and energy absorption on nose landing gear.

which is equal to the 5.5 deg standard condition and the associated aircraft pitching motions. Because of the main gear influence, the energy transfer does result in somewhat reduced loads at the lower sinking speeds, but the effect is relatively small.

Effect of Variation of Moment of Inertia in Pitch I

This is shown in Fig. 8. The variable used is actually the radius of gyration, which is related to the pitching moment of inertia by $k = \sqrt{(I/W)}$.

It is no surprise (first graph, Fig. 8) to find that the aircraft responds more rapidly when the pitching inertia is relatively small. However, what is of great interest is that the vertical forces are almost unchanged at the times when the nose gear touches and develops its maximum values. Although the timing is affected, the positions where the similar loads are felt are scarcely altered. With the exception of main gear compression at nose gear touchdown, this lack of variation is generally true on this aircraft and landing gear combination.

For the nose gear, however, the effect of reduced pitching inertia increases the speed of its initial touchdown but reduces the associated force. This result is not so easy to understand, in view of the occurrence of greater sinking speeds with the low values of pitching inertia. The energy absorbed there does have a local minimum within the range of radius of gyration that was considered, but the effect is relatively small, and it appears that the associated aircraft motion combines with the inertia effect to reduce its overall influence at the nose.

Effect of Variation of Aircraft Size W

The measure for scale is taken here as the mass compared to that of the baseline aircraft. As explained earlier, there are a number of input quantities that must be varied together, to cover the changes due to this parametric variable. Unlike the earlier sets of results, where the output was expressed directly in the resulting physical units, it is convenient here to normalize these values with a factor that converts them to the scale of the baseline aircraft. For the input parameters, these conversions were described earlier, and for the output quantities, they are applied as follows. The linear dimensions are taken to the fifth root of the scale, and the forces are taken to the four-fifths root of the scale. Then the product of the two results in

the energy being in direct proportion to it. In Fig. 9, the particular parameter has been indicated by a prime to show these adjustments. The results are described below.

The effect on the timing is nonlinear, and as expected, the smaller aircraft have the fastest responses. The maximum loads on the main gears appear to follow closely the given scaling laws, but, at the times when the nose gear is being included, it is apparent that the smaller scale of aircraft have an advantage in their loads being of a smaller proportion. The pitch-angle response is almost unaffected by scale except at the instant of nose gear touchdown, when the smaller aircraft have greater angles. However their lift/weight ratios become progressively smaller with reduced scale, due to a greater overall angular response.

Of interest is the local minimum in main gear shock absorber compression at about the scale of the baseline aircraft, but as far as energy absorption is concerned, there is a greater proportion taken in the main gears, when the scale is reduced. For the nose gear, there appears to be a continuous and useful reduction in sinking speed with diminishing scale, but until it has reduced by more than one-eighth of the baseline, the relative forces on this gear do not usefully decrease to any greater advantage, an effect that only applies to the results at the smallest scale that was taken. Both the scaled values of compression of these gears and their relative energy absorption requirements are advantageous, as the size reduces. The implication of all this is that, for the large scale of aircraft, the effects on the nose gears become especially significant, and it is here that the effects of the combined pitch and heave motion should be taken most seriously.

Equivalent Mass at the Nose Gear

As was previously seen in the analysis by Chester[5] and in flight testing by Chester and Brot,[6] the explanation for the relatively large and apparently out of proportion forces on the nose gear is due to its equivalent mass W_e. This artificial quantity is considerably greater than the "static" mass at the nose, due to the contribution to it of the effects of the pitching moment of inertia. For each simulation run, the value of this equivalent mass was determined by equating the nose gear kinetic energy $\frac{1}{2}W_e(z_{n1})^2$ at the time of its impact, with the total strain energy when the gear is fully compressed.

Note how the ratio of equivalent to "static" mass changes with the variation of the input parameters used. These results are shown in Fig. 10. In Fig. 10a, when the initial pitch angle T_{η_0} is about 4.5 deg, there is a maximum energy transfer effect, from the overall pitching motion of the aircraft during the landing operation. This initial angular setting affects the distribution of the kinetic energies between the nose and main gears; smaller and greater settings both tend to reduce the relative amount of energy that passes to the nose. This is because, at the greater initial pitch angles, the height of the center of gravity reduces the effect of the moment arm of the main gear and the angular motion is lessened. At angular settings closer to the case of level landing, the nose gear is more able to respond with an opposing moment, before a large pitching motion has developed on the aircraft.

In Fig. 10b, the effect of the initial sinking speed V_{ss} on the equivalent mass is seen to be minor. This is because the motion in pitch is derived from the initial landing-impact conditions, but the relative motion of pitching compared to heaving remains almost the same.

In Fig. 10c, the pitching radius of gyration is seen as being of great significance to the value of the equivalent/static mass ratio, having a linear variation with it. Over a specific time interval, the amount of transferred energy is virtually independent of the pitching moment of inertia because, with reductions in size of this quantity, the motion becomes more lively (Fig. 8) and the speed of impact grows. Consequently, we would expect a parabolic relationship between the equivalent mass and the radius of gyration because $k = \sqrt{(I/W)}$, with W unchanged. However, as already noted, the time taken for the nose impact to occur is also reduced with the smaller inertia in pitch I. Thus, in terms of the amount of energy that is actually absorbed, the varied pitch inertia has a multiple effect. It is this product that straightens the curve.

In Fig. 10d, a number of these effects are combined, and it is impossible to separate them. This is why the simulation program was

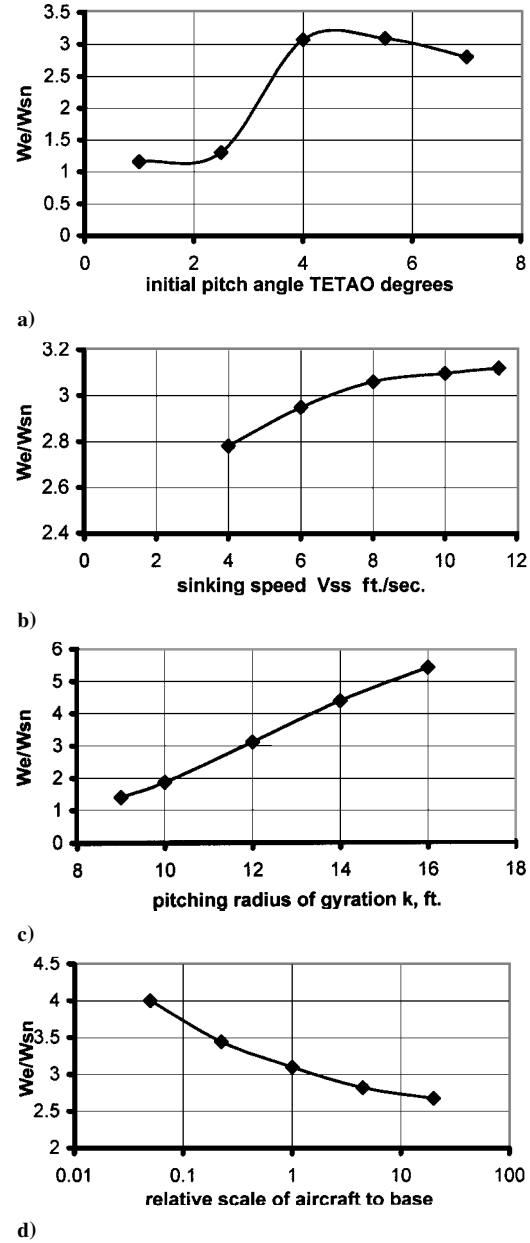

Fig. 10 Influence on the ratio of equivalent/static mass with a) T_{η_0}, b) V_{ss}, c) k, and d) aircraft scale.

developed, rather than trying to perform a simpler kind of analysis. The main trend clearly shows that as the scale of the aircraft is reduced the importance of the concept of equivalent mass grows, although it is significant at all scales.

Evidence supporting these findings was provided in Refs. 3, 6, and 7. In Ref. 6, an analytic approach was used to find the equivalent mass, which was compared to some test results of the Airbus B1 and F104G airplanes in Ref. 3. In Ref. 7, the results of flight testing of Israel Aircraft Industries Galaxy and Saab SF-340 airplanes were presented, for use in developing a fatigue spectrum. These data confirmed the relationships of pitching inertia to the equivalent masses.

Summary/Conclusions

A parametric approach to simulation of landing impact with two degrees of freedom of the aircraft motion (in pitch and heave) has been used to determine the response of the main and nose gears. The results are for comparison to the dynamic behavior of each gear when it is treated as operating independently, as is commonly assumed.

It was found that there are differences in the landing conditions and in the resulting vertical loads and displacements of the gears

when the aircraft motion is included. For main gears, the maximum vertical loads are almost linearly dependent on the sinking speed, but the energy absorbed sometimes exceeds the initial kinetic energy due to potential energy effects. Except for energy transfer to the nose, which subsequently tends to reduce the load, the main gear response may be reasonably predicted by single gear analysis.

However, for the nose gear, the results of this simulation are inconsistent with the single gear assumptions. In particular, it was found that there is no correlation with aircraft sinking speed. Also, the response of nose gears has been found to be very sensitive to the values of initial pitch angle and pitching inertia. This is partly due to the equivalent mass at the nose being greatly affected by these input quantities and by the aircraft scale.

Level landings are uncommon occurrences but are frequently employed as design criteria. Depending on the nose gear situation, the design criteria based on these kinds of landings alone are insufficient to cover the most severe conditions of impact.

References

[1]"Airworthiness Standards: Transport Category Airplanes," Pt. 25, *Code of Federal Regulations—Aeronautics and Space*, Vol. 14, Office of the Federal Register National Archives and Records Administration, Jan. 1998, pp. 361–366, 382–384.

[2]"Airworthiness Standards: Normal, Utility, Acrobatic and Computer Category Airplanes," Pt. 23, *Code of Federal Regulations—Aeronautics and Space*, Vol. 14, Office of the Federal Register National Archives and Records Administration, Jan. 1988, pp. 200–204, 221–224.

[3]Buxbaum, O., "Landing Gear Loads of Civil Transport Airplanes," *8th Plantema Memorial Lecture, Proceedings of the 11th International Committee on Aeronautical Fatigue Symposium*, 1981, pp. 0/1–0/36.

[4]Micklos, R. P., "Landing Parameter Surveys of Transport Aircraft," *Proceedings of the U.S. Air Force Structural Integrity Program Conference*, 1996, pp. 307–334.

[5]Nelson, R. S., Nelson, R. K., and Bland, J., "Avoiding Airplane Damage on Nose Gear Touchdown," *Airliner*, Customer Service Div., Boeing Commercial Airplane Group, The Boeing Co., Seattle, WA, April–June 1994, pp. 22–25.

[6]Chester, D. H., "The Equivalent Masses at Nose Landing-Gears During Landing Impacts and When Crossing Runway Perturbations," *Israel Journal of Technology*, Vol. 23, 1986/1987, pp. 25–31.

[7]Chester, D. H., and Brot, A., "Development of a Fatigue-Spectrum for the Nose Landing-Gear Impact on the GALAXY Executive Jet," *Proceedings of the 20th International Committee on Aeronautical Fatigue Symposium*, 1999, pp. 811–824.